

INTERPRETATION OF GRAVITY ANOMALY DATA USING THE WAVELET TRANSFORM MODULUS MAXIMA

Tin Duong Quoc Chanh^{1,2*}, Dau Duong Hieu¹, Vinh Tran Xuan¹

¹Can Tho University, Vietnam

²PhD student of University of Science, VNU Ho Chi Minh city, Vietnam

*E-mail: dqctin@ctu.edu.vn

Received: 9-11-2017

ABSTRACT: Recently, the continuous wavelet transform has been applied for analysis of potential field data, to determine accurately the position for the anomaly sources and their properties. For gravity anomaly of adjacent sources, they always superimpose upon each other not only in the spatial domain but also in the frequency domain, making the identification of these sources significantly problematic. In this paper, a new mother wavelet function for effective analysis of the locations of the close potential field sources is used. By theoretical modeling, using the wavelet transform modulus maxima (WTMM) method, the relative function between the wavelet scale factor and the depth of gravity source is set up. In addition, the scale parameter normalization in the wavelet coefficients is reconstructed to enhance resolution for the separation of these sources in the scalogram, getting easy detection of their depth. After verifying the reliability of the proposed method on the theoretical models, a process for the location of the adjacent gravity sources using the wavelet transform is presented, and then applied for analyzing the gravity data in the Mekong Delta. The results of this interpretation are consistent with previously published results, but the level of resolution for this technique is quite coincidental with other methods using different geological data.

Keywords: Analysis of potential field data, gravity anomalies of adjacent sources, relative function, scale normalization, wavelet transform modulus maxima method.

INTRODUCTION

Wavelet transforms originated in geophysics in the early 1980s for the analysis of seismic signals [1]. Since then, considerable mathematical advances in wavelet theory have enabled a suite of applications in numerous fields. In geophysics, wavelet has been becoming a very useful tool because of its outstanding capabilities in interpreting nonstationary processes that contain multiscale features, detection of singularities, explanation of transient phenomena, fractal and multifractal processes, signal compression, and some others

[1-4]. It is anticipated that in the near future, significant further advances in understanding and modeling geophysical processes will result from the use of wavelet analysis [1]. A sizable area of geophysics has inherited the achievement of wavelet analysis that is interpretation of potential field data. In this section, it was applied to noise filtering, separating of local or regional anomalies from the measurement field, determining the location of homogeneous sources and their properties [5]. Recently, Li et al., (2013) [6] used the continuous wavelet transform based on complex Morlet wavelet function, which had

been developed to estimate the source distribution of potential fields. The research group built an approximate linear relationship between the pseudo-wavenumber and source depth, and then they established this method on the actual gravity data. However, moving from wavelet coefficient domain to pseudo-wavenumber field is quite complicated and takes a lot of time for calculation as well as analysis. In this paper, for a better delineation of source depths, a correlative function between the gravity anomaly source depth and the wavelet scale parameter has been developed by our synthetic example. After discussing the performance of our technique on various source types, we adopt this method on gravity data in the Mekong Delta, Southern Vietnam to define the adjacent sources distribution.

THEORETICAL BACKGROUND

The continuous wavelet transform and Farshad - Sailhac wavelet function

The continuous wavelet transform (CWT) of 1D signal $f(x) \in L^2(R)$ can be given by:

$$\begin{aligned}
 W(a,b) &= \frac{1}{\sqrt{a}} \int_{-\infty}^{+\infty} f(x)\bar{\psi}\left(\frac{b-x}{a}\right)dx \\
 &= \frac{1}{\sqrt{a}} (f * \bar{\psi})
 \end{aligned}
 \tag{1}$$

Where: $a, b \in R^+$ are scale and translation (shift) parameters, respectively; $L^2(R)$ is the Hilbert space of 1D wave functions having finite energy; $\bar{\psi}(x)$ is the complex conjugate function of $\psi(x)$, an analyzing function inside the integral (1), $f * \bar{\psi}$ expresses convolution integral of $f(x)$ and $\bar{\psi}(x)$. In particular, CWT can operate with various complex wavelet functions, if the wavelet function curve looks like the same form of the original signal.

To determine horizontal location and the depth of the gravity anomaly sources, the complex wavelet function called Farshad - Sailhac [7] was used. It is given by:

$$\psi^{(FS)}(x) = \psi^{(F)}(x) + i\psi^{(S)}(x)
 \tag{2}$$

Where:

$$\psi^{(F)}(x) = \frac{4 - 2x^2}{(x^2 + 2^2)^{\frac{5}{2}}} - \frac{1 - 2x^2}{(x^2 + 1^2)^{\frac{5}{2}}}
 \tag{3}$$

$$\psi^{(S)}(x) = Hilbert(\psi^{(F)}(x))
 \tag{4}$$

The wavelet transform modulus maxima (WTMM) method

Edge detection technique using the CWT was proposed by Mallat and Hwang (1992) [8] correlated to construction of the module contours of the CWT coefficients for analysed signals. To apply this technique, the implemented wavelet functions should be produced from the first or second derivative of a feature function which was related to transfer of potential field in the invert problems. Farshad - Sailhac wavelet function was proven to satisfy the requirements of the Mallat and Hwang method, so the calculation, analysis and interpretation for horizontal position as well as the depth of the regions having strong gravity anomalies were counted on the module component of the wavelet transform. The edge detection technique was based on the locations of the maximum points of the CWT coefficients in the scalogram. Accordingly, the edge detection technique using CWT was also called the “wavelet transform modulus maxima” method.

Yansun Xu et al., (1994) [9] performed wavelet calculations on the gradient of the data signal to denoise and enhance the contrast in the edge detection method using CWT technique. This helps to detect the location of small anomalies alongside the large sources better because the gradient data has the property of amplifying the instantaneous variations of the signal. Therefore, in the following sections, we apply wavelet transformations on gradient gravity anomaly instead of applying them on gravity anomaly to analyze the theoretical models and then apply for actual data.

Determination of structural index

We denote $f(x, z=0)$ as measured data in the ground due to a homogeneous source located at $x=0$ and $z=z_0$ with the structural index N . When we carry out the continuous wavelet transform on the $f(x, z=0)$ with the wavelet functions that are the horizontal derivative of kernel in the upward field transposition formula, the equation related to the wavelet coefficients at two scale levels a and a' is obtained:

$$W_{f(x,z=0)}^\gamma(x, a) = \left(\frac{a}{a'}\right)^\gamma \left(\frac{a'+z_0}{a+z_0}\right)^{-\beta} W_{f(x,z=0)}^\gamma(x', a') \quad (5)$$

Where: x and a are position and scale parameters, respectively; β indicates the uniform level of the singular sources; γ illustrates the order of derivatives of analyzing wavelet functions.

According to Sailhac et al., (2000) [10], with the unified objects having equally distributed mass, causing gravity anomaly, the relationship between N , β , and γ is given by following formula: $N = -\beta - \gamma - 2$ (6).

For different positions x and x' , the connection of scale parameters a and a' is given as follows:

$$\frac{a'+z_0}{x'} = \frac{a+z_0}{x} = const \quad (7)$$

In this paper, the structural index N of anomaly sources is determined by Farshad - Sailhac wavelet function with $\gamma=2$, thus the equation (5) can be rewritten as follows:

$$\begin{aligned} & \left(\frac{1}{a}\right)^2 W_{f(x,z=0)}^2(x, a)(a+z_0)^{-\beta} \\ & = \left(\frac{1}{a'}\right)^2 W_{f(x,z=0)}^2(x', a')(a'+z_0)^{-\beta} \quad (8) \\ & = const \end{aligned}$$

Using short notation $W_{f(x,z=0)}^2(x, a) = W_2(x, a)$ and taking the logarithm on both sides of equation (8), a new expression is derived:

$$\log\left(\frac{W_2(x, a)}{a^2}\right) = \beta \log(a+z_0) + c \quad (9)$$

Where: c is constant related to the *const* in the right side of equation (8). Therefore, the determination of structural index is done by the estimation on the slope of a straight line:

$$Y = \beta.X + c \quad (10)$$

Where: $Y = \log\left(\frac{W_2(x, a)}{a^2}\right)$ and $X = \log(a+z_0)$.

By determining the structural index, we can estimate the relative shapes of the gravity anomaly sources.

The wavelet scale normalization

Basically, for the adjacent sources making gravity anomalies, the superposition of total intensity from gravity fields is related to different factors such as: position, depth, and the size of component sources. In this case, the wavelet maxima that are associated with bigger anomalies in the scalograms of wavelet coefficient modulus often dominates those associated with smaller anomalies, making the identification of gravity sources problematic. To overcome the aforementioned problems, the wavelet scale normalization scheme is applied to shorten the gap of wavelet transform coefficient modulus in the scalogram between the large anomalies and small ones. Thus, facilitating location of adjacent sources is easy to estimate, especially for small ones.

To separate potential field of adjacent sources from the scalogram, a scale normalization a^{-n} on the 1D continuous wavelet transform (equation (1)) has been introduced. Then the normalized 1-D CWT can be expressed as:

$$W'(a, b) = a^{-n} \int_{-\infty}^{+\infty} f(x) \frac{1}{\sqrt{a}} \bar{\psi}\left(\frac{b-x}{a}\right) dx \quad (11)$$

Where: n is a positive constant. When $n = 0$, there is no scale normalization, and the equation (11) returns to equation (1). As analyzing some simple gravity anomalies, using the Farshad - SAILHAC wavelet function, n can take values from 0 to 1.5. When n increases, wavelet transform coefficient $W'(a,b)$ in equation (11) decreases and the ratio of modulus wavelet coefficient contributed by the large and small anomalies in the scalogram reduces. Then, the resolution on the figure is also improved so much. In this article, the value $n = 1.5$ (the highest resolution) is selected for the potential field interpretation of modeling data of adjacent sources as well as actual data.

The relationship between scale and source depth

In general, a scale value in the wavelet transform relates to the depth of anomaly sources. However, it is not the depth and does not provide a direct intuitive interpretation of depth. To interpret the scalogram through the theoretical models with the sources built by the distinct shaped gravity objects, a close linear correlation between the source depth z and the

product of scale a and measured step Δ is shown with the normalizing factor k :

$$z = k.(a.\Delta) \tag{12}$$

The normalizing factor k in the equation (11) comes from the structural index N of the source. In the results and discussions, this factor k will be determined and applied to estimate the depth of the singular sources for the measured data.

RESULTS AND DISCUSSIONS

Theoretical models

Model 1: Simple anomaly sources

In this model, the gravity source is homogeneous sphere with the radius of 1 km, put in a unified environment. The different mass density between the anomaly object and the environment is 3.0 kg/dm^3 . The sphere center is located at horizontal coordination $x = 15 \text{ km}$ and vertical coordination $z = 3.0 \text{ km}$. The measurement on the ground goes through the sphere, with total length of 30 km , having step size of $\Delta = 0.1 \text{ km}$. Fig. 1a and fig. 1b are the total intensity gravity anomaly and the gradient of the total intensity gravity anomaly caused by the sphere in turn.

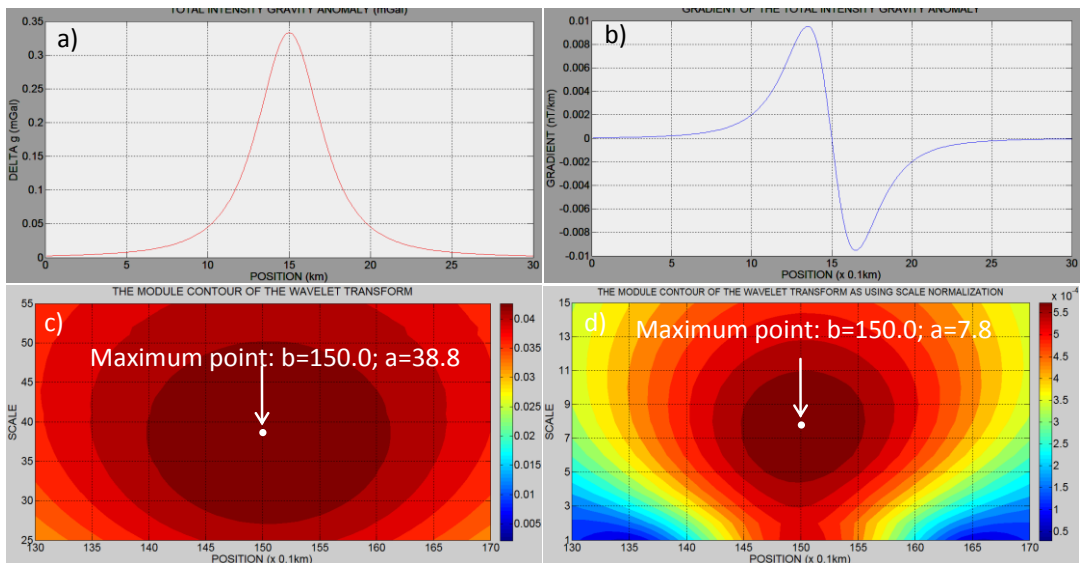


Fig. 1. The graphs of the model 1: a) The total gravity anomaly intensity, b) The gradient of the total gravity anomaly intensity, c) The module contours of the wavelet transform, d) The module contours of the wavelet transform as using scale normalization

According to the results plotted by module in fig. 1c or fig. 1d, we easily found the maximum point of the wavelet transform coefficients located at $(b=150.0; a=38.8)$ or $(b=150.0; a'=7.8)$. To multiply value b with measured step $\Delta=0.1$ km, the horizontal location of the source center will be identified: $x=150.0 \times 0.1=15$ km. This value of x is accordant with the parameter of the model. Therefore, the modulus maxima in the wavelet

scalogram are capable of identifying the source horizontal position.

The value of the scaling factor $a=38.8$ or $a'=7.8$ is related to the source depth. To find the correlative function between the depth z and scaling factor a or a' , we take the value of z from 1.0 to 9.0 km and repeat the survey process as well as $z=3$ km. The survey results are represented in table 1 and fig. 2.

Table 1. Analytical results with Farshad - Sailhac wavelet function

| z (km) | Δ (km) | a ($n=0$) | $(a.\Delta)$ | a' ($n=1,5$) | $(a'.\Delta)$ |
|----------|---------------|---------------|--------------|------------------|---------------|
| 1.5 | 0.1 | 19.4 | 1.94 | 3.8 | 0.38 |
| 2.0 | 0.1 | 25.8 | 2.58 | 5.0 | 0.50 |
| 2.5 | 0.1 | 32.4 | 3.24 | 6.4 | 0.64 |
| 3.0 | 0.1 | 38.8 | 3.88 | 7.8 | 0.78 |
| 3.5 | 0.1 | 45.0 | 4.50 | 9.0 | 0.90 |
| 4.0 | 0.1 | 51.5 | 5.14 | 10.2 | 1.02 |
| 4.5 | 0.1 | 58.0 | 5.80 | 11.6 | 1.16 |
| 5.0 | 0.1 | 64.4 | 6.44 | 12.8 | 1.28 |
| 5.5 | 0.1 | 70.8 | 7.08 | 14.2 | 1.42 |
| 6.0 | 0.1 | 77.2 | 7.72 | 15.4 | 1.54 |
| 6.5 | 0.1 | 83.6 | 8.36 | 16.6 | 1.66 |
| 7.0 | 0.1 | 90.0 | 9.00 | 17.8 | 1.78 |
| 7.5 | 0.1 | 96.4 | 9.64 | 19.0 | 1.90 |
| 8.0 | 0.1 | 102.8 | 10.28 | 20.4 | 2.04 |
| 8.5 | 0.1 | 109.4 | 10.94 | 21.6 | 2.16 |
| 9.0 | 0.1 | 115.6 | 11.56 | 23.0 | 2.30 |

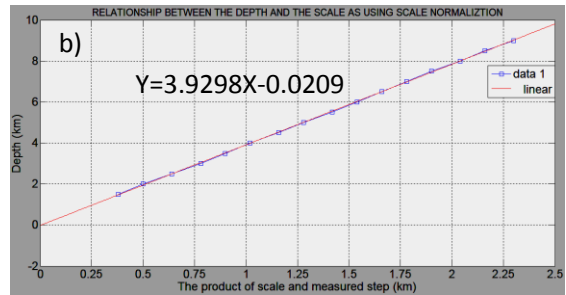
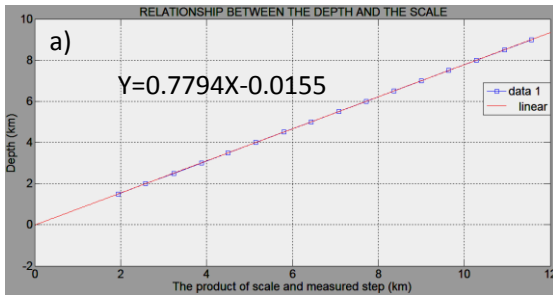


Fig. 2. The relationship between the depth and the product of scale and measured step: a) no scale normalization, b) using scale normalization

As can be seen in fig. 2, we determine the approximate linear relationship between the

scale parameter and gravity source depth:

$$z \approx 0.7794 \times (a.\Delta) \text{ (km)} \quad \text{as no scale normalization} \quad (13)$$

$$z \approx 3.9298 \times (a'.\Delta) \text{ (km)} \quad \text{as using scale normalization with } n = 1.5 \quad (14)$$

When gravity sources are far away from the observation plane, they are usually assumed as spheres [6]. Then the relative source depths can be estimated from the maximum points of the CWT coefficients in the scalogram by equation (13) or (14).

In fact, other simple sources, such as cube,

cylinder, prism, long sheet, step, were used widely in the real measurement. Thus, it is necessary to check our method with different forms of sources instead of spherical form. Testing results of the normalizing factor k or k' corresponding to different shaped sources are presented in table 2.

Table 2. Structural index N and equivalent parameter k or k'

| Shaped source | Structural index N | k | k' |
|-------------------|----------------------|--------|--------|
| Sphere or cube | 2 | 0.7794 | 3.9298 |
| Cylinder or prism | 1 | 0.6280 | 3.5215 |
| Long sheet | $0 < N < 1$ | 0.2288 | 2.4899 |
| Step | 0 | 0.1863 | 1.9512 |

Model 2: Adjacent anomaly sources

We consider the total gravity field anomaly produced by two homogeneous cylinders, put in a unified environment. The different mass densities between the anomaly objects and the environment are the same -8.5 kg/dm^3 . The cylinder 1 has a radius of 2 km and is located at horizontal coordination $x = 22 \text{ km}$ and vertical coordination $z = 3.2 \text{ km}$, while the cylinder 2 is

situated at horizontal coordination $x = 7 \text{ km}$ and vertical coordination $z = 1.8 \text{ km}$ with a radius of 0.5 km. The measurement on the ground goes through those anomaly objects, with total length of 30 km, having step size of $\Delta = 0.1 \text{ km}$. Fig. 3a and fig. 3b are the total intensity gravity anomaly and the gradient of the total intensity gravity anomaly caused by two cylinder, respectively.

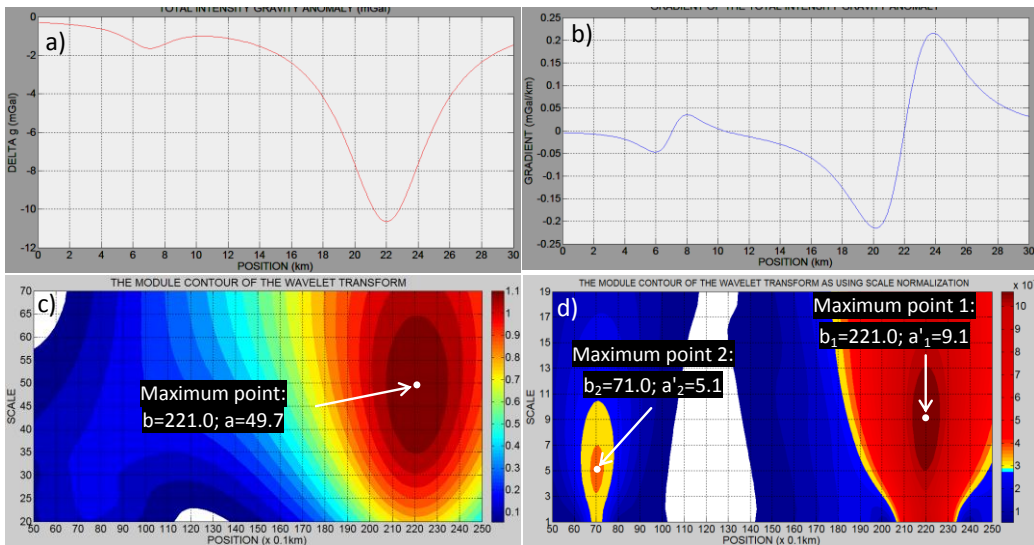


Fig. 3. The graphs of the model 2: a) The total gravity anomaly intensity, b) The gradient of the total gravity anomaly intensity, c) The module contours of the wavelet transform, d) The module contours of the wavelet transform as using scale normalization

As can be seen in fig. 3c, one maximum point of the wavelet transform coefficients is

found at $(b = 221.0; a = 49.7)$ corresponding to position of the cylinder 1 (large anomaly).

Therefore, in this model, for applying the method as model 1 only, we get a difficult problem to identify position of the cylinder 2 (small anomaly) because of the significantly strong effect of the gravity field from the cylinder 1.

To solve this problem, we used the scale normalization in the continuous wavelet transform (equation 10) on the gradient of the total gravity field anomaly produced by two objects. The plotting results of this module in fig. 3d show two maximum points of the wavelet transform coefficients corresponding to anomaly sources, they are situated at: $(b_1 = 221.0; a_1' = 9.1)$ and $(b_2 = 71.0; a_2' = 5.1)$. Then, the horizontal and vertical locations of the center anomaly sources will be identified: $x_1 = 221.0 \times 0.1 = 22.1$ km; $x_2 = 71.0 \times 0.1 = 7.1$ km; $z_1 = 3.5215 \times 0.1 \times 9.1 = 3.2$ km; $z_2 = 3.5215 \times 0.1 \times 5.1 = 1.8$ km. These values of x and z are accordant with parameters of the model. Therefore, the modulus maxima in the wavelet scalogram and scale normalization are capable of identifying the location of adjacent sources.

From good results as analyzing the theoretical models, we have developed a process for determining the location of adjacent anomalous sources, and then applied for actual data.

The process to determine the location of the adjacent sources from gravity anomaly data using Farshad - Sailhac wavelet transform

The determination of the horizontal position and depth of the gravity singular sources using Farshad - Sailhac wavelet transform can be summarized in the process including the following steps:

Step 1: Taking the horizontal gradient of the gravity anomaly along the measured profile.

Step 2: Performing Farshad - Sailhac wavelet transform on the horizontal gradient of the gravity anomaly data.

After carrying out complex CWT, there are four distinct data sets: real part, virtual component, module factor, and phase

ingredient. The module data will be used in the next step.

Step 3: Changing the different scales a and repeating the multiscale CWT.

Step 4: Plotting the module contours by the CWT coefficients with different scales a in the scalogram (a, b) .

Step 5: Determining the position of the gravity anomaly sources.

On the wavelet scalogram of module contours, finding the maximum points of the wavelet transform coefficients. The horizontal and vertical coordinates of these points are b_i and a_i , respectively (where i expresses numerical order of the sources). The position of the sources will be determined by following equation:

$$x_i = b_i \times \Delta \tag{15}$$

Step 6: Detecting the depth of the gravity anomaly sources.

Calculating the structural index of the anomaly sources identified in step 5 and estimating the relative shape of the sources. Then, determining k_i or k_i' factors from table 2. The depth of the sources will be detected by following equation:

$$z_i = k_i \cdot (a_i \cdot \Delta) \text{ as no scale normalization} \tag{16}$$

$$z_i = k_i' \cdot (a_i' \cdot \Delta) \text{ as using scale normalization} \tag{17}$$

Analysis of the gravity data from the Mekong Delta

Applying the process for the location of the gravity singular sources using Farshad - Sailhac wavelet transform to analyze actual data, we have interpreted some of measured profiles on the map of Bouguer gravity anomaly in the Mekong Delta. The map at 1/100,000 scale is provided by the Southern Geological Mapping Federation, which was measured and completed in 2006.

The analysis results are highly accurate and fairly compliant with the previous publication of the geological data. Nevertheless, in this

paper, the research group only shows the interpretation results for Ca Mau profile. Ca Mau negative anomaly (latitude $9^{\circ}15'N$ -longitude $105^{\circ}04'E$) has a axis deviation -30° from the north. The singular source is about 20 km wide and 30 km long. The minimum of

anomaly values is -10 mGal. The survey profile (Southwest - Northeast) goes through the center of the anomaly source and cuts straight to the axis of the singular source. It has 31 km long, and step size of 1.0 km (fig 4a).

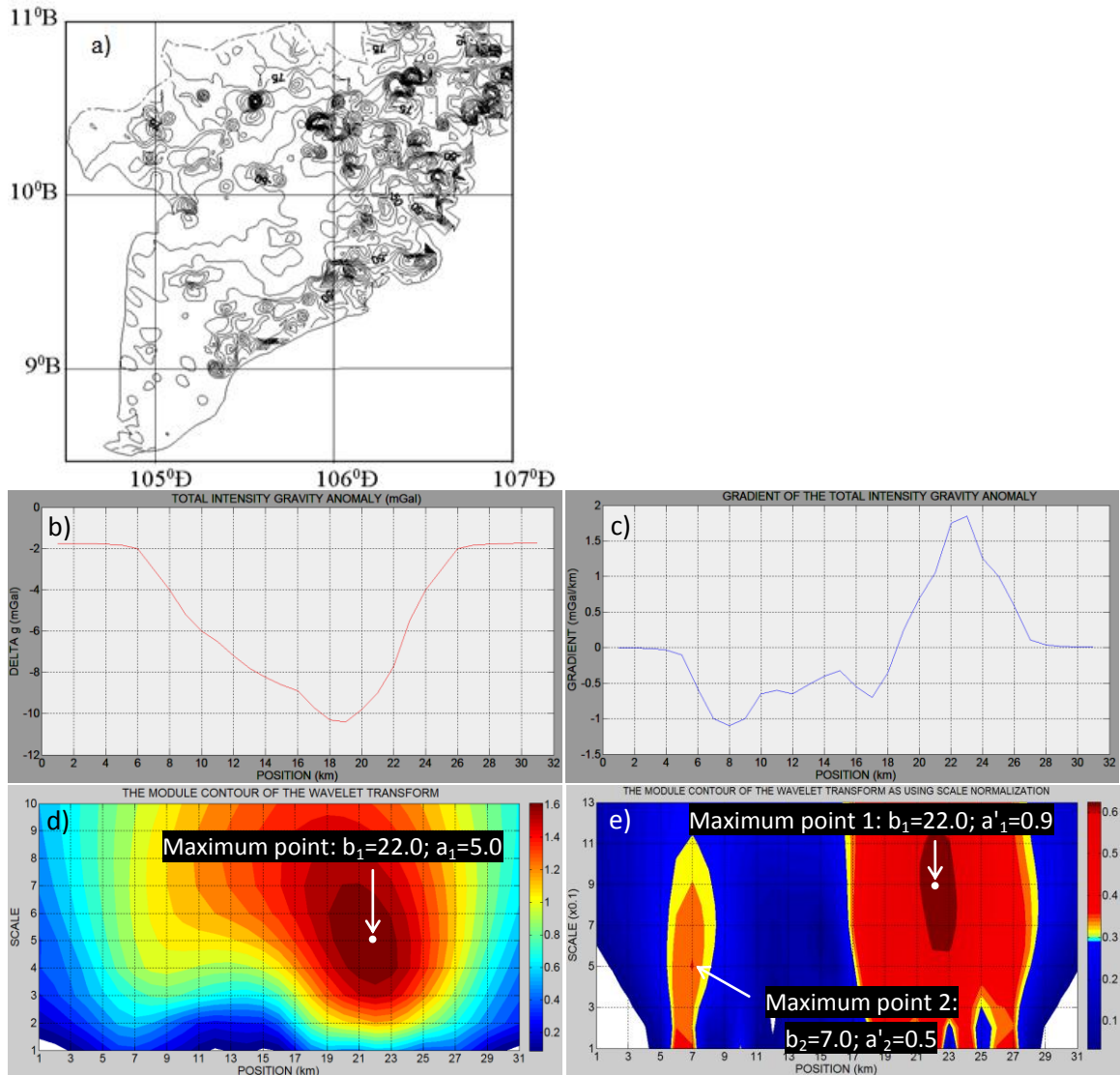


Fig. 4. The graphs of actual data: a) The profile survey on the map of Bouguer gravity anomaly, b) The total gravity anomaly intensity, c) The gradient of the total gravity anomaly intensity, d) The module contours of the wavelet transform, e) The module contours of the wavelet transform as using scale normalization

Fig. 4b and fig. 4c are the total gravity anomaly intensity and the gradient of the total gravity anomaly intensity along the profile in

turn, in which one strong anomaly is at position 22^{nd} km.

From fig. 4d, there is only one the maximum point of the wavelet transform coefficients corresponding to the larger source from the strong anomaly, and it is situated at: $x_1 = 22$ (km), $a_1 = 5.0$.

The scale normalization in the continuous wavelet transform (equation 11) on the gradient of the total gravity anomaly field of the profile is used. The plotting results of this module in fig. 4e show two maximum points of the wavelet transform coefficients corresponding to two anomaly sources, they are situated at: ($b_1 = 22.0$; $a_1 = 0.9$) and ($b_2 = 7.0$; $a_2 = 0.5$).

Fig. 5b is the logarithm curve of wavelet

transform $\log(W/a^2)$ with logarithm of $(a+z)$ of the anomaly source located at position of 22 km. Using the least square method to determine the equation of linear line: $Y = -5.1X + 8.1$, so $\beta \approx -5$ (equation 10), thus, the structural index is $N = 5 - 2 - 2 = 1$ (equation 6). Consequently, the source may be a cylinder or prism and the normalizing factor $k = 0.6280$ or $k' = 3.5215$ (table 2). To multiply the normalizing factor k with $(a_1 \cdot \Delta)$ or k' with $(a_1 \cdot \Delta)$, the depth of the source at 22nd km would be detected, it was about 3.2 km. To take a similar analysis for the other anomaly on the profile, the summarized results in table 3 are obtained.

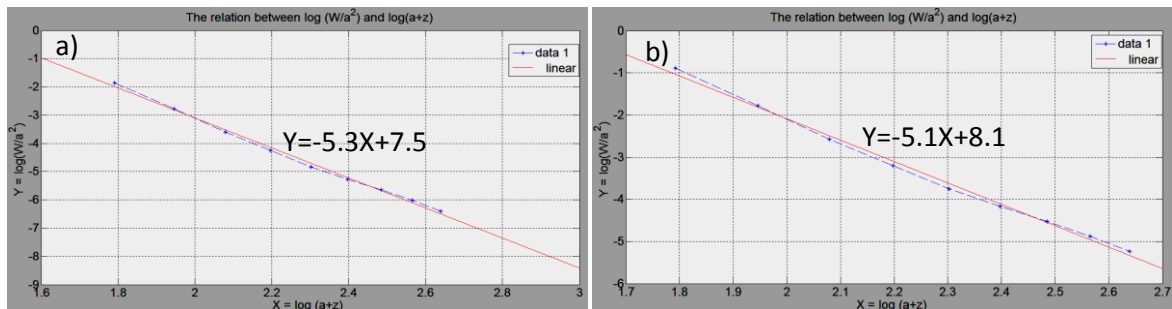


Fig. 5. The graphs of the relation between $\log(W/a^2)$ and $\log(a+z)$:
 a) anomaly source 2nd at 7th km, b) anomaly source 1st at 22nd km

Table 3. The results of interpretation of Ca Mau profile

| Anomaly source No. | Horizontal position (km) | Uniform level β | Structural index N | Relative shape | Depth (km) |
|--------------------|--------------------------|-----------------------|----------------------|-------------------|------------|
| 1 | 22 | 5 | 1 | Cylinder or prism | 3.2 |
| 2 | 7 | 5 | 1 | Cylinder or prism | 1.8 |

CONCLUSIONS

In this paper, a new mother wavelet namely Farshad - Sailhac is used to solve the potential field inverse problems to determine the horizontal position, depth and structural index of the gravity anomaly sources. The wavelet scale normalization is applied to enhance the resolution for the separation of these sources in the scalograms, and it is a better method to identify their location, especially for small sources. Through the analysis of theoretical models, using the wavelet transform modulus maxima, the correlative function approximate

linear between the source depth and the wavelet scale parameter has been established. Then, the process for the location of the gravity anomaly sources using Farshad - Sailhac wavelet transform has been developed and applied successfully. The results of interpretation on Ca Mau profile illustrate that there are two gravity anomaly sources along the profile, including two cylinders or prisms, with their position, depth and structural index being quite coincident with the previously published geological results [11].

REFERENCES

1. Kumar, P., and Foufoula-Georgiou, E., 1997. Wavelet analysis for geophysical applications. *Reviews of Geophysics*, **35**(4), 385-412.
2. Ouadfeul, S., 2006. Automatic lithofacies segmentation using the wavelet transform modulus maxima lines (WTMM) combined with the detrended fluctuation analysis (DFA). *17th International Geophysical Congress and Exhibition of Turkey*, Expanded abstract.
3. Ouadfeul, S., 2007. Very fines layers delimitation using the wavelet transform modulus maxima lines WTMM combined with the DWT. *SEG SRW*, Expanded abstract.
4. Ouadfeul, S. A., Aliouane, L., and Eladj, S., 2010. Multiscale analysis of geomagnetic data using the continuous wavelet transform: a case study from Hoggar (Algeria). In *2010 SEG Annual Meeting. Society of Exploration Geophysicists*.
5. Fedi, M., and Quarta, T., 1998. Wavelet analysis for the regional-residual and local separation of potential field anomalies. *Geophysical prospecting*, **46**(5), 507-525.
6. Li, Y., Braitenberg, C., and Yang, Y., 2013. Interpretation of gravity data by the continuous wavelet transform: The case of the Chad lineament (North-Central Africa). *Journal of Applied Geophysics*, **90**, 62-70.
7. Tin, D. Q. C., and Dau, D. H., 2016. Interpretation of the geomagnetic anomaly sources in the Mekong Delta using the wavelet transform modulus maxima. *Workshop on Capacity Building on Geophysical Technology in Mineral Exploration and Assessment on Land, Sea and Island, Hanoi*, Pp. 121-128.
8. Mallat, S., and Hwang, W. L., 1992. Singularity detection and processing with wavelets. *IEEE transactions on information theory*, **38**(2), 617-643.
9. Xu, Y., Weaver, J. B., Healy, D. M., and Lu, J., 1994. Wavelet transform domain filters: a spatially selective noise filtration technique. *IEEE transactions on image processing*, **3**(6), 747-758.
10. Sailhac, P., Galdeano, A., Gibert, D., Moreau, F., and Delor, C., 2000. Identification of sources of potential fields with the continuous wavelet transform: Complex wavelets and application to aeromagnetic profiles in French Guiana. *Journal of Geophysical Research: Solid Earth*, **105**(B8), 19455-19475.
11. Dau, D. H., 2013. Interpretation of geomagnetic and gravity data using continuous wavelet transform. *Vietnam National University Ho Chi Minh city Press*, Pp. 127.